URSI-RCRS 2024, ARIES/GEHU, Bhimtal, India, 22 - 25 October, 2024

Evolution of Warm Cloud Effective Radius using Multi-Satellite Observations

Sijo Joseph[1]*, Subin Jose[1] and N.B. Lakshmi[2]
(1) Department of Physics, Newman College, Thodupuzha, Kerala, India
(2) National Centre for Earth Observation, University of Leicester, Leicester, UK
*sijojoseph@newmancollege.ac.in

Abstract

This paper investigates the influence of aerosols on cloud microphysical growth using SUOMI-VIIRS and CALIPSO satellite observations collocated in space and time. By considering the vertical evolution of cloud and aerosol layers, we use simultaneously observed cloud and aerosol data to examine cloud microphysical growth under various aerosol loading conditions. Aerosol loading cases were classified based on the aerosol optical depth (AOD). Low aerosol loading is defined as an AOD of less than 0.2, moderate aerosol loading as $0.2 \leq AOD \leq 0.5$, and high aerosol loading as greater than 0.5. This study revealed the dominance of diffusional growth over collision-coalescence growth in high aerosol loading conditions. We also estimated the mean cloud droplet growth rate ($-dr_e/dT$) in different aerosol loading conditions. Mean cloud droplet growth in the low aerosol loading case shows a high value (0.41), which is higher than in moderate (0.36) and high (0.02) aerosol loading conditions. Furthermore, using linear regression analysis, we investigated the relationship between cloud growth and stability measures under different aerosol conditions. The results show that the linear Pearson coefficient between the lifting condensation level and Estimated Inversion Strength is significant and high (r = 0.61) in high aerosol loading conditions compared to low (r = 0.44) and moderate (r = 0.47) aerosol loading conditions.

1. Introduction

Effects of aerosols on microphysical properties of clouds are among the key components that influence the Earth's climate [1] ..Aerosols serve as cloud condensation nuclei (CCN) upon which cloud droplets can be formed. Human activity has led to an increase in atmospheric aerosols, in turn increasing the supply of CCN nuclei which can change

cloud properties. If the cloud water available for condensation remains constant, will result in a higher number of small droplets and consequently, a higher albedo [2]. This effect is called the first indirect effect (Twomey/albedo effect). Albrecht argued that a decrease in size of cloud droplets would retard rain formation and increase the cloud lifetime. This hypothesis is known as second indirect effect (Albrecht/lifetime effect) [3].
Despite years of studies, it is still difficult to establish meaningful relationships between aerosol, cloud, and precipitation [4]. Aerosol-Cloud Interaction (ACI) depends on two regimes: cloud regimes and meteorological regimes. The challenge of disentangling meteorology from aerosol effects on cloud properties in the boundary layer can be addressed by retrieving cloud microphysical and thermodynamic properties along with aerosol observations [5][1]. Significant efforts have been going on to understand which effect is dominant (thermodynamic or aerosol effects). An understanding of vertical microstructure of the clouds helps in determining the thermodynamics of the clouds. Different clouds clusters have different cloud properties such as cloud top height (CTH), cloud top temperature (CTT) and droplet size defined by the Cloud Droplet Effective Radius (r_e), which is the ratio of the total volume of all drops in a particular region divided by the total surface area [6]. Changes in the droplet size, r_e in clouds is an important climate parameter as it can influence climate sensitivity. The vertical evolution of CDER (re), is an important parameter in representing the microphysical characteristics of clouds [7].

Cloud properties change with respect to changes in aerosol and meteorological cloud controlling factors [8]. Increased aerosol loading (taking AOD as proxy) modifies cloud microphysics by changing cloud droplet size with height. More small droplets can delay the onset of precipitation, thus allows cloud droplets to be carried to higher levels, increasing the amount of condensed water within the cloud, thus increasing evaporation at cloud top and moistening/cooling the layer above the cloud, hence destabilizing the cloud top region [9][4]. Cloud formation usually takes place in rising air, which expands and cools, thus permitting the activation of aerosol particles into cloud droplets and ice crystals in supersaturated air [1]. Microphysical classification of clouds from base to top includes zones of diffusional growth, coalescence growth, rainout zone, mixed zone and glaciation [10]. Precipitation efficiency will be higher in clean case (aerosol limited regime) than in the polluted case (updraft-limited regime). [11], from their satellite and radar analysis found a value of 14μm for r_e as the precipitation threshold for dominant collision and coalescence processes and it denotes the separation point of precipitating and non-precipitating clouds.

Cloud regimes can be defined based on the cloud properties which provides a powerful method for representing the state of the atmosphere. If the relationship between aerosol and cloud changes greatly under different meteorological regimes, it suggests that meteorological variables play an important role in modulating aerosol-cloud interaction [12]. The local meteorology can be characterized by the stability of the boundary layer [13] and the meteorological variable we used for this estimation is Estimated Inversion Strength (EIS) [14].

2. Data and Methodology

(a) Data

Multispectral analysis of satellite images are used to analyze clouds. We utilized observations from the Suomi National Polar-orbiting Partnership (Suomi-NPP) to analyze the cloud droplet growth with height. Suomi-NPP is a joint satellite mission between NASA and NOAA, equipped with various instruments, including the Visible Infrared Imaging Radiometer Suite (VIIRS), which provides valuable data for studying cloud properties. Simultaneously, aerosol vertical profiles of these regions are identified by Cloud-Aerosol Lidar Infrared Pathfinder Satellite Observations (CALIPSO). CALIPSO is a joint satellite mission between NASA and the French Space Agency, CNES. Further we plotted potential temperature, relative humidity and specific humidity profiles to estimate EIS, which is a measure of atmospheric stability of that region, using Suomi-NPP CrIS data. Aerosol optical Depth (AOD) can be estimated from the Visible Infrared Imaging Radiometer Suite (VIIRS) NASA standard Level-3 (L3) daily Deep Blue aerosol products from the Suomi National Polar-orbiting Partnership (SNPP) instrument.

(b) Methodology

The interaction between aerosols and clouds can be examined using the methodology introduced by [10]. Using the quantitative methodology introduced by [10], Cloud Top Temperature (T, K) versus Cloud drop effective Radius (r_e, μm) curves are plotted to identify the cloud microphysical processes in different aerosol loading cases. The Initial step involves defining a window containing a cloud cluster with elements representing all growth stages. Then different percentiles (15, 50, 85) of r_e are calculated for each 1°C interval of cloud-top temperature. The shape of the T-r_e profiles contains much information about the different microphysical processes in the cloud system such as (a) diffusion and condensational growth (b) coalescence growth (c) rainout (d) mixed phase and (e) glaciated zone. These processes are identified at different heights. The aerosol extinction coefficient, i.e., the sum of the scattering and absorption by aerosol particles, varies with altitude above the surface. The distribution of aerosols in the atmosphere can be different at different vertical levels. Scene selection was designed to maximize the number of aerosol and low-level cloud observations while excluding high-level cloud. Aerosol extinction coefficient profiles are derived from CALIPSO data.

EIS, a refined metric than Lower Tropospheric Stability (LTS) which is estimated by measuring the difference in potential temperature between 700hPa and the surface level (Wood & Bretherton, 2006). EIS is calculated by the equation mentioned below

$$EIS = LTS - \tau_M^{850}(Z_{700} - LCL) \quad (1)$$

where τ_M^{850} is the moist adiabatic potential temperature gradient, Z_{700} is the height at 700 hPa level and LCL is the lifting condensation level.

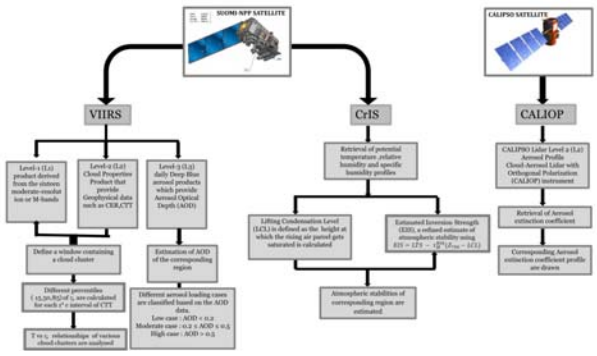

Figure 1. Schematic presentation of methodology used in the study.

3. Results

3.1 Cloud Growth under different Aerosol Loading Conditions (Low, Moderate and High cases)

In this study AOD < 0.2 is defined as a case of low aerosol loading case. An AOD value between 0.2 < AOD <0.5 is considered a moderate aerosol loading case, while an AOD > 0.5 is classified as a high aerosol loading case.

(i) Low aerosol loading case: Analysis reveals the existence of different microphysical processes in different aerosol-loaded cases. Figure 2 depicts that for low aerosol loading case, there is a rapid increase in Cloud drop effective radius (r_e) with height (CTT) and exceeds 14μm precipitation threshold at short distance above cloud base. From Table 1 we can observe the mean Droplet growth rate ($-dr_e/dT$) to be 0.41 which is higher than moderate and high aerosol loading cases. This implies that the collision-coalescence process dominates over the diffusion process.

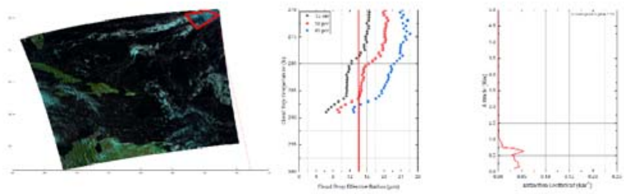

Figure 2. Cloud growth under low aerosol loading case (AOD < 0.2). (a) NPP/VIIRS high resolution (375m) image of the analyzed area and (b) T versus r_e relationship and aerosol vertical distribution profile of the regions. The red vertical bar at 14µm denotes precipitation threshold.

(ii) Moderate aerosol loading case: Figure 3 showing that r_e increases more slowly with height compared to low aerosol loading case. The presence of more numerous but smaller droplets delays the onset of precipitation, which is evident from the slower rise in r_e. The mean cloud droplet growth rate was estimated as 0.36.

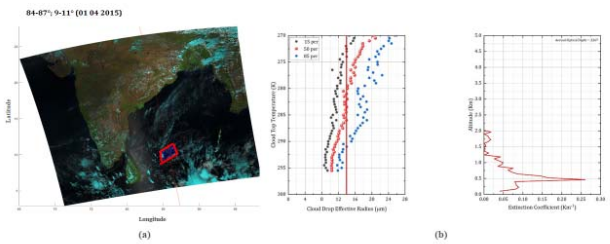

Figure 3. Cloud growth under moderate aerosol loading case (0.2 ≤ AOD ≤ 0.5). (a) NPP/VIIRS high resolution (375m) image of the analyzed area and (b) T versus r_e relationship and aerosol vertical distribution profile of the regions. The red vertical bar at 14µm denotes precipitation threshold.

(iii) High aerosol loading case: Figure 4 shows that the r_e profiles are more uniform and exhibit less variability with height. In this case, the cloud droplets remain small due to the high concentration of aerosols, which suppresses the collision-coalescence process. The r_e does not reach the 14µm threshold as quickly as in the low and moderate cases, indicating a reduced efficiency in precipitation formation. The least mean cloud droplet growth rate (0.02) can be observed in this case. This uniformity suggests that microphysical processes such as condensational growth are more dominant in highly polluted environments, where aerosol loading can be seen above the boundary layer.

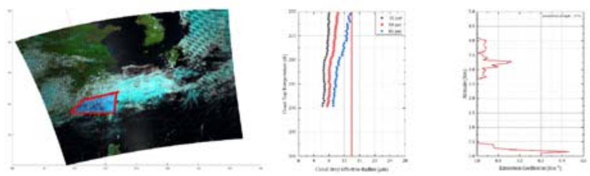

Figure 4. Cloud growth under high aerosol loading case (AOD > 0.5). (a) shows NPP/VIIRS high resolution (375m) image of the analyzed area and (b) T versus r_e relationship and aerosol vertical distribution profile of the regions. The red vertical bar at 14µm denotes precipitation threshold.

Table 1. Mean cloud droplet growth rate ($-dr_e/dT$) under different aerosol loading cases

Aerosol loading case	Mean ($-dr_e/dT$)
Low	0.41
Moderate	0.36
High	0.02

3.2 The Relationship between Cloud Growth and Stability Measures in different Aerosol Conditions

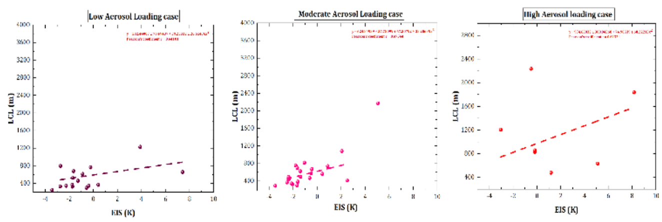

Figure 5. Relationship between Lifting Condensation Level (LCL) and EIS in each aerosol loading cases

The relationship between the Estimated Inversion Strength (EIS) and the Lifting Condensation Level (LCL) (Figure 5) is critical in understanding boundary layer dynamics and cloud formation processes. LCL can be used as a reasonable estimate of cloud base height. Aerosol loading, which can vary from low to high, significantly influences this relationship. Linear regression analysis has been carried out between cloud base height (CBH) and the measure of stability (EIS) and linear Pearson correlation coefficient is given in Table 2.

Table 2. Linear Pearson Correlation Coefficients between LCL and EIS

Aerosol loading cases	r
Low	0.44
Moderate	0.47
High	0.61

From Table 2 we can observe that the correlation coefficient between LCL and EIS in high aerosol loading cases is high (r= 0.61) compared to low (r = 0.44) and moderate (r = 0.47) aerosol loading cases. This implies that as aerosol loading increases, the influence of atmospheric stability on cloud properties becomes more pronounced.

4. Conclusions

The cloud droplet growth rate exhibits significant variation across different aerosol loading cases, underscoring the critical role of aerosol concentration in determining cloud microstructure. Our findings indicate that condensational growth becomes the dominant process as aerosol loading increases. This study reveals that cloud properties and their growth mechanisms are notably influenced by the stability of the atmosphere in varying aerosol conditions. Specifically, the mean cloud droplet growth rate is highest in low aerosol loading conditions ($AOD < 0.2$) and decreases progressively in moderate ($0.2 \leq AOD \leq 0.5$) and high ($AOD > 0.5$) aerosol conditions. Additionally, the strong positive correlation ($r = 0.61$) between the Lifting Condensation Level and Estimated Inversion Strength, in high aerosol loading scenarios, highlights the impact of aerosols on cloud stability measures. These insights are crucial for improving our understanding of cloud-aerosol interactions and refining atmospheric models to better predict weather and climate phenomena.

5. Acknowledgements

The work has been supported by the Science and Engineering Research Board (SERB), DST, Govt. of India, under the Project Code: SRG/2022/001537.We are also grateful to the NOAA Science team for supplying satellite data. We acknowledge the facilities and support provided by management of Newman College, Thodupuzha, Kerala.

6. References

1. Randall, D., Artaxo, P., Bretherton, C., Feingold, G., Forster, P., Kerminen, V., Kondo, Y., Liao, H., Lohmann, U., Rasch, P., Satheesh, S., Sherwood, S., Stevens, B., Zhang, X., Qin, D., Plattner, G., Tignor, M., Allen, S., Boschung, J., … Randall, D. (2013). *Clouds and Aerosols. In: Climate Change 2013: The Physical Science Basis. Contribution of Working Group I to the Fifth Assessment Report of the Intergovernmental Panel on Climate Change Coordinating Lead Authors: Lead Authors*.
2. Twomey, S. (1977). The Influence of Pollution on the Shortwave Albedo of Clouds. In *Journal of the Atmospheric Sciences* (Vol. 34, Issue 7, pp. 1149–1152). https://doi.org/10.1175/15200469(1977)034<1149:tiopot >2.0.co;2
3. Albrecht, B. A. (1989), Aerosols, cloud microphysics, and fractional cloudiness, Science, 245(4923), 1227–1230, doi:10.1126/science.245.4923.1227.
4. Stevens, B., & Feingold, G. (2009). Untangling aerosol effects on clouds and precipitation in a buffered system. In *Nature* (Vol. 461, Issue 7264, pp. 607–613). https://doi.org/10.1038/nature08281
5. Rosenfeld, D., et al. "The scientific basis for a satellite mission to retrieve CCN concentrations and their impacts on convective clouds." Atmospheric Measurement Techniques 5.8 (2012): 2039-2055.
6. Rosenfeld, D., & Woodley, W. (2001). Pollution and clouds. *Physics World*, *14*(2), 33–37. https://doi.org/10.1088/2058-7058/14/2/30
7. Chen, Y., Chen, G., Cui, C., Zhang, A., Wan, R., Zhou, S., Wang, D., & Fu, Y. (2020). Retrieval of the vertical evolution of the cloud effective radius from the Chinese FY-4 (Feng Yun 4) next-generation geostationary satellites. *Atmospheric Chemistry and Physics*, *20*(2), 1131–1145. https://doi.org/10.5194/acp-20-1131-2020
8. Rosenfeld, D., Kokhanovsky, A., Goren, T., Gryspeerdt, E., Hasekamp, O., Jia, H., et al. (2023). *Frontiers in satellite-based estimates of cloud-mediated aerosol forcing*. Reviews of Geophysics, 61, e2022RG000799. https://doi.org/https://doi. org/10.1029/2022RG000799
9. Rosenfeld, D. (2000). Suppression of rain and snow by urban and industrial air pollution. *Science*, *287*(5459), 1793–1796. https://doi.org/10.1126/science.287.5459.1793.
10. Lensky, I. M., & Rosenfeld, D. (1998). Satellite-based insights into precipitation formation processes in continental and maritime convective clouds at nighttime. *Journal of Applied Meteorology*, *42*(9), 1227–1233. https://doi.org/10.1175/1520-0450(2003)042<1227:SIIPF P >2.0.CO;2.
11. Rosenfeld, D., & Gutman, G. (1994). Retrieving microphysical properties near the tops of potential rain clouds by multispectral analysis of AVHRR data. *Atmospheric Research*, *34*(1–4), 259–283. https://doi.org/10.1016/0169-8095(94)90096-5
12. Lin, Y., Takano, Y., Gu, Y., Wang, Y., Zhou, S., Zhang, T., Zhu, K., Wang, J., Zhao, B., Chen, G., Zhang, D., Fu, R., & Seinfeld, J. (2023). Characterization of the aerosol vertical distributions and their impacts on warm clouds based on multi-year ARM observations. *Science of the Total Environment*, *904*(June). https://doi.org/10.1016/j.scitotenv.2023.166582.
13. Douglas, A., & L'Ecuyer, T. (2020). Quantifying cloud adjustments and the radiative forcing due to aerosol-cloud interactions in satellite observations of warm marine clouds. *Atmospheric Chemistry and Physics*, *20*(10), 6225–6241. https://doi.org/10.5194/acp-20-6225-2020.
14. Wood, R., & Bretherton, C. S. (2006). On the relationship between stratiform low cloud cover and lower-tropospheric stability. *Journal of Climate*, *19*(24), 6425–6432. https://doi.org/10.1175/JCLI3988.1.